

# RSC Advances



This article can be cited before page numbers have been issued, to do this please use: A. Ghorbani-Choghmarani, M. Hajjami, A. A. Derakhshan and L. Rajabi, *RSC Adv.*, 2016, DOI: 10.1039/C6RA19725F.



This is an *Accepted Manuscript*, which has been through the Royal Society of Chemistry peer review process and has been accepted for publication.

*Accepted Manuscripts* are published online shortly after acceptance, before technical editing, formatting and proof reading. Using this free service, authors can make their results available to the community, in citable form, before we publish the edited article. This *Accepted Manuscript* will be replaced by the edited, formatted and paginated article as soon as this is available.

You can find more information about *Accepted Manuscripts* in the [Information for Authors](#).

Please note that technical editing may introduce minor changes to the text and/or graphics, which may alter content. The journal's standard [Terms & Conditions](#) and the [Ethical guidelines](#) still apply. In no event shall the Royal Society of Chemistry be held responsible for any errors or omissions in this *Accepted Manuscript* or any consequences arising from the use of any information it contains.



## RSC Advanced

## Paper

Received 00th January  
20xx,

## Copper-Schiff base alumoxane: a new and reusable mesoporous nano catalyst for Suzuki–Miyaura and Stille C–C cross-coupling reactions

Accepted 00th January 20xx

Arash Ghorbani-Choghamarani,<sup>a\*</sup> Ali Ashraf Derakhshan,<sup>a</sup> Maryam Hajjami<sup>a</sup> and Laleh Rajabi<sup>b</sup>

DOI: 10.1039/x0xx00000x

[www.rsc.org/](http://www.rsc.org/)

Herein for the first time, a mesoporous copper nano catalyst (SBA-Cu<sup>2+</sup>) were simply synthesized through immobilization of Cu<sup>2+</sup> on surface of Schiff base alumoxane support. This nano catalyst was characterized by various techniques such as FT-IR, X-ray Map, TG-DTA, BET, SEM, SEM-EDS, TEM, ICP-OES and XRD. The characterization results indicated that SBA-Cu<sup>2+</sup> nanoflakes with 331.47 m<sup>2</sup> g<sup>-1</sup> specific surface area are thermally stable up to 306 °C. The SBA-Cu<sup>2+</sup> nano catalysts showed significant activity for Suzuki–Miyaura and Stille cross-coupling reactions with good efficiency and reusability. In addition, the nanocatalyst can be recovered and reused several times without significant loss of its catalytic activity. Copper leaching from SBA-Cu<sup>2+</sup> is very negligible for this coupling reaction.

### 1. Introduction

C–C bond construction is one of the most important chemical transformations which can be used in the production of many man-made products [1]. Over past decades, The Suzuki–Miyaura and Stille cross-coupling reactions have been utilized as powerful methodologies in C(sp<sup>2</sup>)–C(sp<sup>2</sup>) bond formation [2]. In this field, the homogeneous palladium as the most suitable and widely used catalyst has shown high yields, good selectivity and convenient turnover numbers [3].

Despite the widespread applications as a catalyst, the homogeneous Pd complexes have the limiting aspects such as toxicity and high price which led to limitation of them on industrial scale applications [4]. As a viable alternative for Pd, recently copper-based catalysts have attracted much attention due to their biocompatibility and lower price as well as their catalytic aptitude for cross-coupling reactions [5]. Despite these advantages, only a few Suzuki or Stille reactions involving copper catalyzed cross-coupling have been reported. These copper based catalysts are including Cu/Schiff-base@Fe<sub>3</sub>O<sub>4</sub> [6], Cu nano colloid [7], 3D MOF {[Cu(4-tba)<sub>2</sub>](solvent)}<sub>n</sub> [8], Cu@molecular sieve [9] and Pd-Cu@Carbon [10]. Thus, to expand the copper catalyzed Suzuki or Stille coupling reactions, the development of new and

efficient nano catalysts based on Cu is necessary. In this way, the use of novel materials as a catalyst support is inevitable. Immobilization of Cu species on solid supports in heterogeneous catalysts facilitates separation, minimizing contamination and reusability of expensive catalysts. In order to preparation of heterogeneous catalysts, various solid supports including polymers, zeolites, silica, carbon nanotubes and metal-organic frameworks (MOFs) have been utilized [11]. The nature of supports can influence the selectivity and reactivity of the catalyst, therefore careful choice of supports can be led to creation of new heterogeneous catalysts. As a new suggestion, the carboxylate-alumoxane is a versatile compound which can be introduced as a novel support for heterogeneous catalysts. Carboxylate alumoxanes with general formula [Al(O)<sub>x</sub>(OH)<sub>y</sub>(O<sub>2</sub>CR)<sub>z</sub>]<sub>n</sub>, 2x+y+z=3 are prepared from the reaction of boehmite (γ-AlOOH) and carboxylic acids. The surface of the alumoxanes is covered with covalently bound carboxylate groups. The physical and chemical properties of the alumoxane can be affected by the type of carboxylic acid, and range from water soluble powders to hard solids that are resistant to acids, bases and organic solvents [12, 13]. As a precursor for alumoxane synthesis, Boehmite is a metastable phase of Aluminium oxide with oxide-hydroxide bonds which commonly used as supporting matrix [14, 15]. The advantages of alumoxane as a catalyst support are included the low price of boehmite and the availability of an almost infinite range of carboxylic acids [16]. The only report on the catalytic use of alumoxane were related to Zirconocene complex supported on para-hydroxybenzoate-alumoxane (PHBA) as novel catalyst for

<sup>a</sup> Chemistry Department, Faculty of Science, Ilam University, Ilam, Iran. \*Email: a.ghorbani@mail.ilam.ac.ir or arashghch58@yahoo.com

<sup>b</sup> Polymer Research Lab., Department of Chemical Engineering, Razi University, Kermanshah, Iran. Email: laleh.rajabi@gmail.com

olefin polymerization [17]. Nevertheless, there is no significant works about application of alumoxanes in the catalysis field especially for C-C coupling reactions.

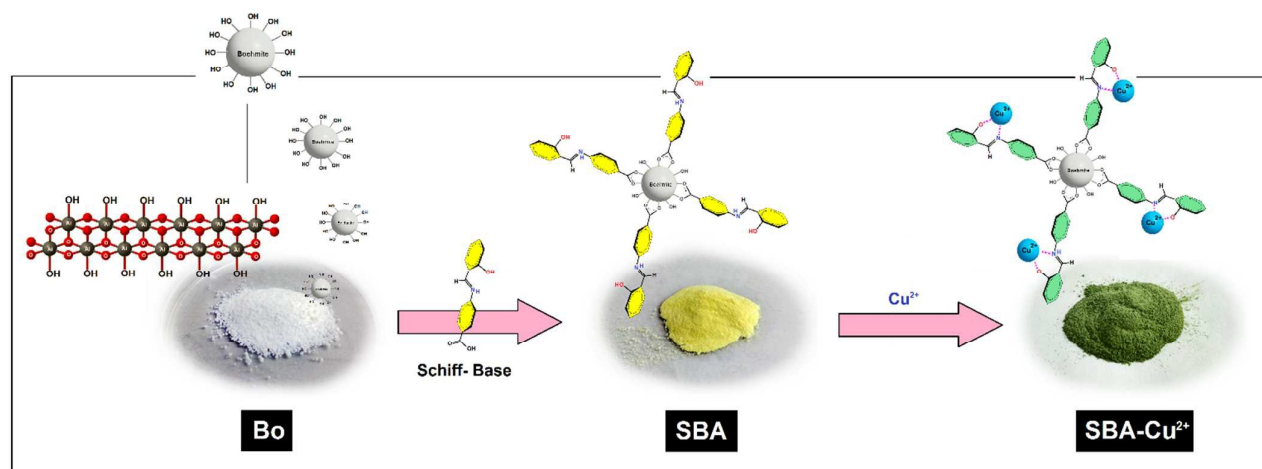


Fig. 1. Stepwise synthesis of Copper-Schiff base Alumoxane (SBA-Cu<sup>2+</sup>) from boehmite schematically.

Currently there is no report about using the alumoxane supports for Suzuki-Miyaura and Stille reactions.

In order to prepare new alumoxane catalysts, Schiff bases ligands can play an important role in complexing of metal cations on alumoxane surface. Therefore the using of carboxylic Schiff-base molecules in the synthesis of alumoxane can be led to formation of novel catalyst support. In this work for the first time we report the successful synthesis of Copper-Alumoxane nano catalyst through immobilization of Cu<sup>2+</sup> on Schiff-base alumoxane and using them as a new nanocatalyst for the Suzuki-Miyaura and Stille coupling reaction (Fig. 1).

## 2. Results and discussion

### 2.1 Catalyst characterization

#### 2.1.1. FT-IR analysis

In order to characterization of molecular structure of organic-inorganic materials, FT-IR spectroscopy can be used as an adequate technique. The FT-IR spectra of the Bo, SBA and SBA-Cu<sup>2+</sup> are provided in Fig. 2. In the Boehmite spectrum (Fig. 2a), the stretching vibration of Al-OH has shown two strong peaks at 3092 and 3316 cm<sup>-1</sup>. Also the hydrogen bonds between Al-OH groups have shown the two peaks (1071 and 1166 cm<sup>-1</sup>) related to the symmetrical bending vibrations. As well as the three peaks of 482, 615 and 741 cm<sup>-1</sup> are related to the vibrational modes of Al-O-Al [14]. The two absorption peaks of 1385 and 1637 cm<sup>-1</sup> are due to the stretching vibration of the NO<sup>3-</sup> impurity and absorbed water in the boehmite structure, respectively.

In the spectrum of SBA (Fig. 2b), there are several peaks in 1200-1800 cm<sup>-1</sup> region which are indicated formation of carboxylate-alumoxane through the covalent bonding between Bo and SB. The two absorption peaks in 1560 and 1492 cm<sup>-1</sup> are related to the asymmetrical and symmetrical stretching vibrations of bidentate carboxylate groups, respectively. As well as the frequency of 1626 cm<sup>-1</sup> is due to unidentate

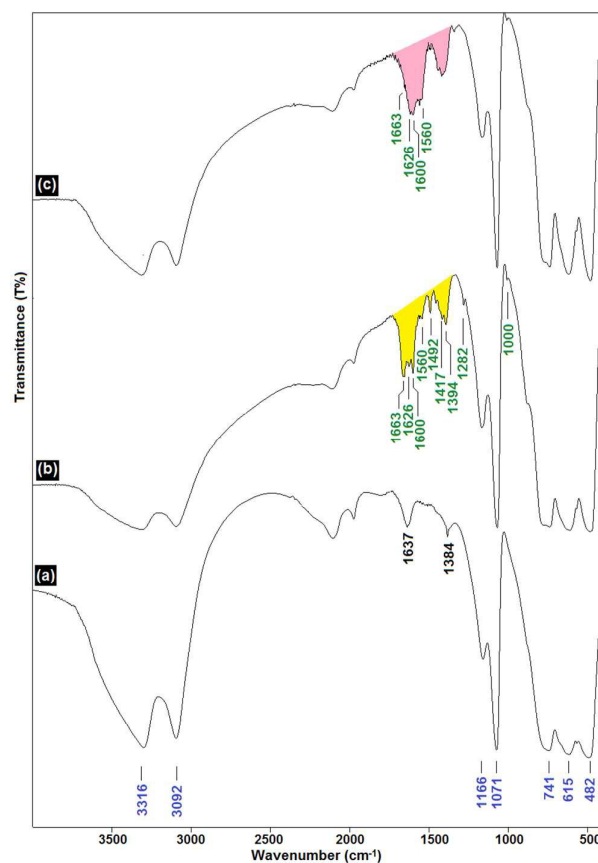


Fig. 2. FT-IR spectra of (a) Bo, (b) SBA and (c) SBA-Cu<sup>2+</sup>

frequency of 1663 cm<sup>-1</sup> while phenolic C-O stretching vibrations are observed at 1282 cm<sup>-1</sup>. Also the two frequencies at 1600 and 1417 cm<sup>-1</sup> are due to the vibrations of sp<sup>2</sup> C=C in the benzene rings [19]. In the spectrum of SBA-Cu<sup>2+</sup> (Fig. 2c),

decreasing in intensity of C=N peak ( $1663\text{ cm}^{-1}$ ) is referred to chelation of  $\text{Cu}^{2+}$  by SBA ligands. It seems that chelation caused to reduce in bond vibrations. Also to increase in peak of  $1560\text{ cm}^{-1}$  can be due to

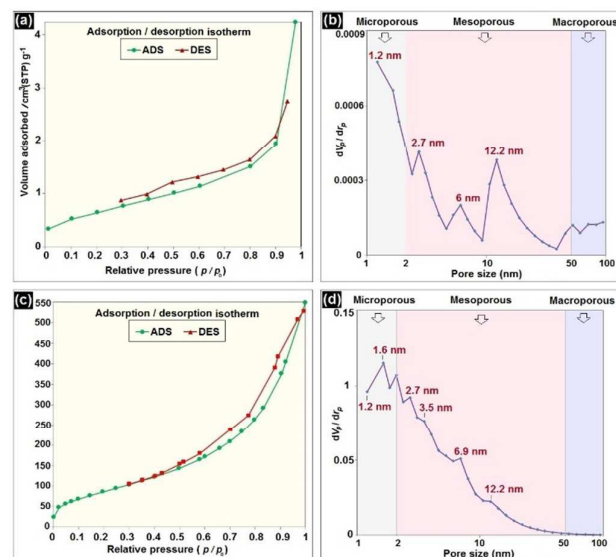


Fig. 3.  $\text{N}_2$  adsorption–desorption isotherms and the corresponding pore size distributions for boehmite nanoparticles (a and b) and  $\text{SBA-Cu}^{2+}$  (c and d).

vibration of acetate ligand which connected to the  $\text{Cu}^{2+}$  [19]. It seems that some of the Al-OH groups in boehmite nanoparticles cannot be reacted with Schiff base SB. Because the boehmite index peaks in SBA and  $\text{SBA-Cu}^{2+}$  spectra have been existence. According to the literature [19], the stretching frequencies of Cu-O and Cu-N emerge at  $431\text{--}455$  and  $555\text{--}470\text{ cm}^{-1}$  for Cu-Schiff base complex. But in the  $\text{SBA-Cu}^{2+}$ , these stretching peaks have covered with overlapping of Al-O-Al stretching modes in the range of  $400\text{--}800\text{ cm}^{-1}$ .

### 2.1.2. Specific surface area analysis

The  $\text{N}_2$  adsorption-desorption isotherms, BET surface area and pore volume of the Bo precursor and  $\text{SBA-Cu}^{2+}$  are shown in Fig. 3. It can be seen from Fig. 3a and Fig. 3c, both of them show type-IV isotherm (defined by IUPAC), which are characterized as mesoporous materials. In Fig. 3 b and Fig. 3d, the pore size distributions are shown micro and meso porosity in the Bo and  $\text{SBA-Cu}^{2+}$  which there is reducing in pore size for  $\text{SBA-Cu}^{2+}$  versus Bo. Table 1 is presented all data attained by Brunauer–Emmett–Teller (BET) and Barrett–Joyner–Halenda (BJH) methods. The specific surface area ( $S_{\text{BET}}$ ) for Bo precursor is  $2.28\text{ m}^2\text{ g}^{-1}$ , with  $22\text{ nm}$  average pore diameter and a specific pore volume of  $0.0125\text{ cm}^3\text{ g}^{-1}$ . Despite of our expectation, Boehmite nano particles (Bo) have shown the very low surface area, which can be due to sever agglomeration among them. In return,  $\text{SBA-Cu}^{2+}$  with the specific surface area ( $S_{\text{BET}}$ ) of  $331.47\text{ m}^2\text{ g}^{-1}$  and average pore diameter  $9.91\text{ nm}$  has shown a specific pore volume of  $0.8217\text{ cm}^3\text{ g}^{-1}$ . It seems that alumoxane formation is caused to reduce in extent of agglomeration and increasing of surface area. The  $D_{\text{av}}$  for boehmite (Bo) and  $\text{SBA-Cu}^{2+}$  illustrated meso porosity while  $D_{\text{BJH}}$  values showed the micro porosity for them.

### 2.1.3. X-ray diffraction

The X-ray diffraction patterns of Bo, SBA and  $\text{SBA-Cu}^{2+}$  are shown in Fig. 4. The low angle XRD patterns (Fig. 4a) only for  $\text{SBA-Cu}^{2+}$  revealed a single intense peak corresponding (100) plan. The other peaks

Table 1. Surface properties of  $\text{SBA-Cu}^{2+}$  and boehmite precursor

Sample	Specific surface area [ $\text{m}^2\text{ g}^{-1}$ ]		Specific pore volume [ $\text{cm}^3\text{ g}^{-1}$ ]		Pore diameter [nm]	
	$S_{\text{BET}}$	$S_{\text{BJH}}$	$V_{\text{tot}}$ (BET)	$V$ (BJH)	$D_{\text{av}}$	$D$ (BJH)
Boehmite	2.28	2.48	0.0125	0.0125	22	1.21
$\text{SBA-Cu}^{2+}$	331.47	397.13	0.8217	0.8404	9.91	1.64

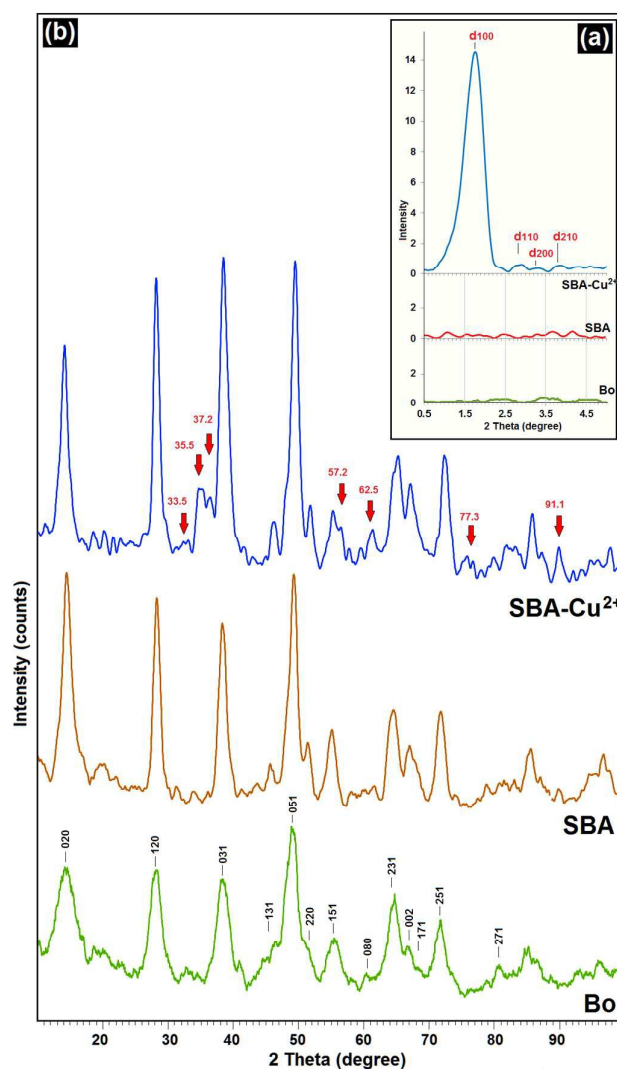


Fig. 4. The low angle (a) and wide angle (b) XRD patterns of Bo, SBA and  $\text{SBA-Cu}^{2+}$

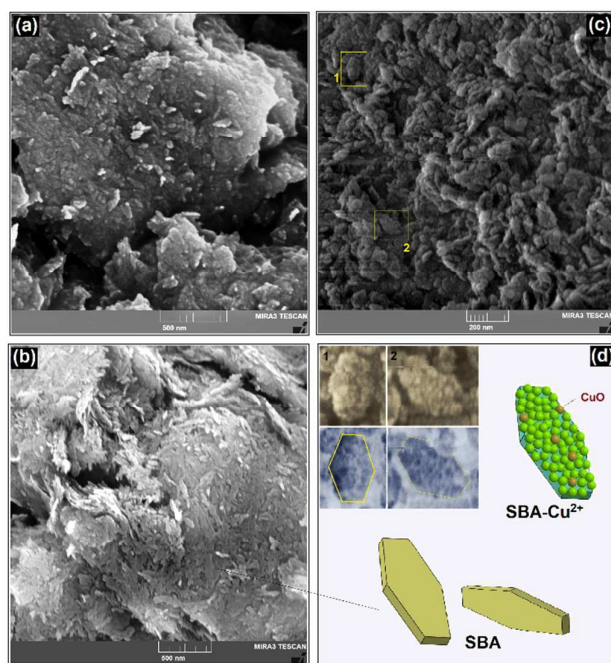


Fig. 5. SEM images of (a) Bo, (b) SBA, (c) SBA-Cu<sup>2+</sup> and (d) schematically morphology of them

72° and 81° which can be attributed to the orthorhombic unit cell of boehmite  $\gamma$ -AlOOH (JCPDS card 21-1307). The Low intensity and broadening peaks shows that Bo nanoparticles had low crystallinity. Just like Bo, the XRD pattern of SBA (Fig. 4b) revealed the same diffraction lines but sharper and more intense than Bo. This may be due to inadequate functionalization of Bo with Schiff-base molecules because of some spherical hindrances. Also increasing in sharpness and intensity of peaks represents its higher crystallinity. In the other hand, the XRD spectrum of SBA-Cu<sup>2+</sup> (Fig. 4b) illustrated the same sharp diffraction peaks of SBA. The emersion of new peaks at  $2\theta = 33.5^\circ, 35.5^\circ, 37.2^\circ, 57.2^\circ, 62.5^\circ, 77.3^\circ$  and  $91.1^\circ$  are related to the Cu<sup>2+</sup> and CuO in the catalyst [20].

#### 2.1.4. SEM and TEM analysis

The SEM images of the parent Bo, SBA and SBA-Cu<sup>2+</sup> are shown in Fig. 5. From Fig. 5(a), it can be seen that Bo sample was included nanoparticles with an average particle size in the range of 10–30 nm. Having surficial OH groups and tendency to hydrogen bonding among them caused to the agglomeration between Bo nanoparticles.

Fig. 5(b) exhibited that the morphology of SBA is significantly different from Bo. The SBA sample has the morphology of irregular nano flakes with about 20-30 nm thickness and 50-100 nm across. It can be seen from Fig. 5(c) the chelation of Cu<sup>2+</sup> by SBA was led to roughen the surface of nano flakes. The magnified images and their schematics illustrate significantly the morphology of SBA-Cu<sup>2+</sup> catalyst (Fig. 5(d)). The TEM images confirmed the morphology of SBA-Cu<sup>2+</sup> and well distribution of Cu<sup>2+</sup> at the surface of mesoporous nano flakes (Fig. 6.). It can be seen that SBA-Cu<sup>2+</sup> has to some extent cubic or hexagonal structures.

The expected elements in the structure of Bo, SBA and SBA-Cu<sup>2+</sup> can be detected by SEM-EDS analysis presented in the Fig. 7. For Bo

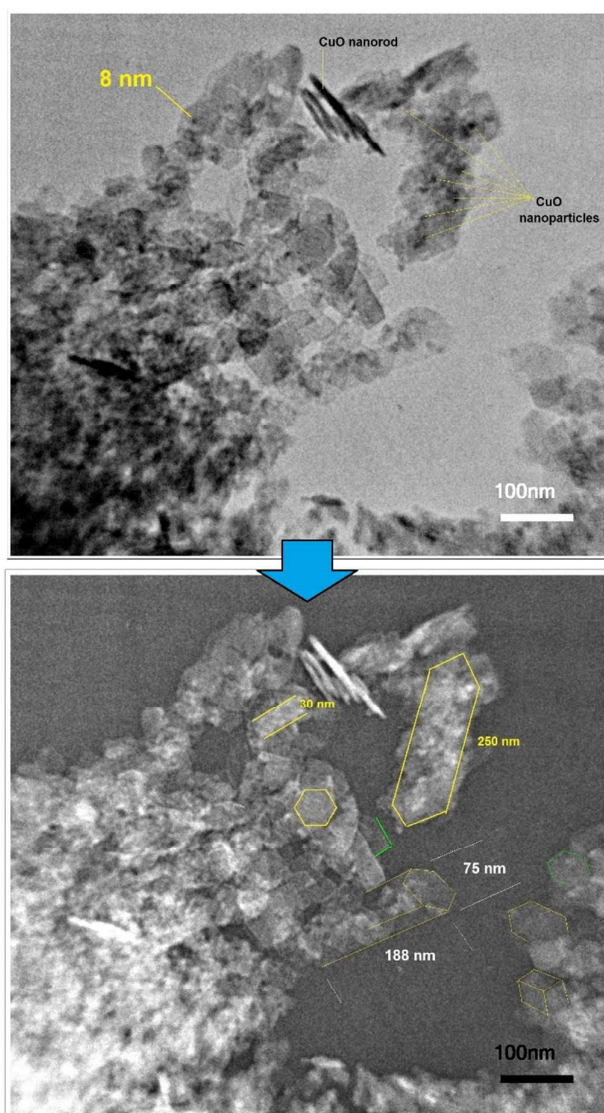


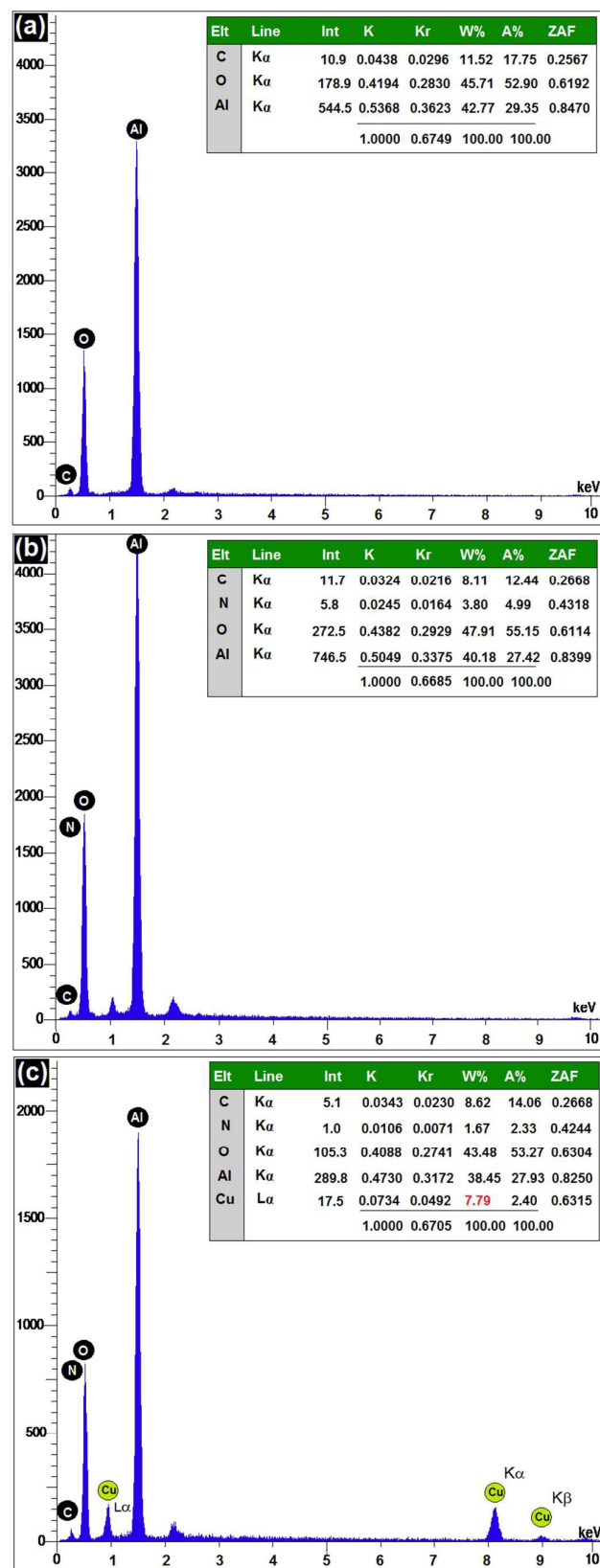
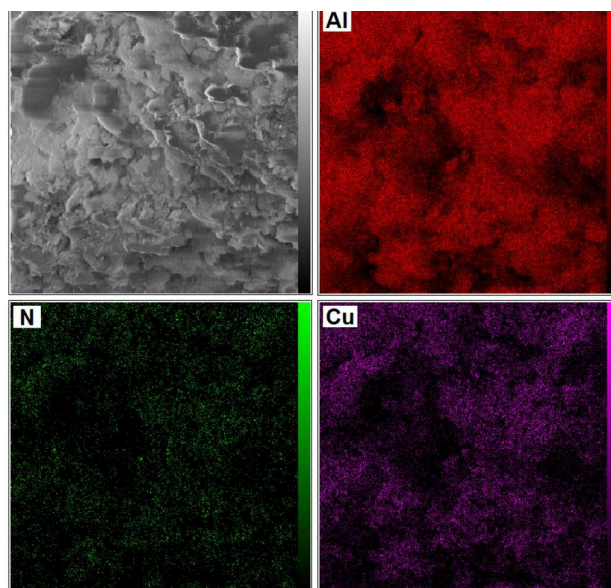
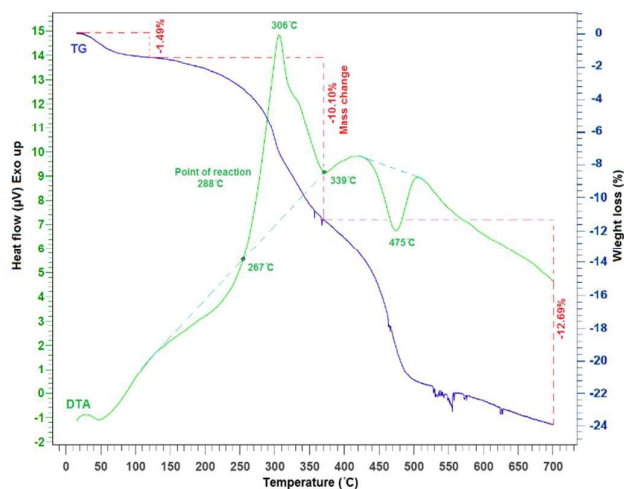
Fig. 6. TEM images of SBA-Cu<sup>2+</sup> nano catalyst

sample the percentage of C, O and Al in Fig. 7(a) have been recorded. In comparing with Bo, The SBA sample shows 3.8 %w for N element which confirms the presence of Schiff-base molecules (Fig. 7(b)). The EDS data for SBA-Cu<sup>2+</sup> also confirms the presence of Cu<sup>2+</sup> on the surface of SBA supports with the weight present about 7.79 %w (Fig. 7c).

The x-ray mapping of SBA-Cu<sup>2+</sup> were recorded in order to evaluate the dispersion of Cu active sites in the catalyst. Fig. 8 shows the elemental map images which confirmed the good dispersion of Cu on surface of catalyst. Also the dispersion of N in the surface are indicated the presence of Schiff-base ligands in the catalyst.

#### 2.1.5. Thermal analysis (TG-DTA)

Thermo gravimetric-differential thermal analysis (TG-DTA) reveals the thermal behavior of the SBA-Cu<sup>2+</sup> nano catalyst. The TG curve in Fig. 9 indicates the three step weight loss that the first step (mass

Fig. 7. SEM-EDS data of (a) Bo, (b) SBA and (c) SBA-Cu<sup>2+</sup>Fig. 8 The x-ray map analysis for SBA-Cu<sup>2+</sup> nano catalystFig. 9. TG-DTA diagrams of SBA-Cu<sup>2+</sup> nano catalyst

The second step weight loss (mass change: 10.1%) is mainly initiated at 267 °C which DTA curve shows an exothermic peak at 306 °C. This step is referred to thermal decomposition of complex. The third step weight loss (mass change: 12.69%) may be related to the phase transfer of boehmite structure to the alumina phase which can be accompanied by OH elimination. Because in SBA-Cu<sup>2+</sup> there are some free Al-OH groups that could not reacted with Schiff-base molecules. For this process, the DTA curve shows an endothermic peak at 475 °C.

## 2.2. Evaluation of catalytic activity

The C-C coupling reactions of aryl halides (Suzuki-Miyaura and Stille reactions) were used to evaluate catalytic performance of SBA-Cu<sup>2+</sup> catalyst.

In our primary experiments, Suzuki–Miyaura reaction between iodobenzene and sodium tetraphenylborate ( $\text{NaBPh}_4$ ) was selected as a model reaction to optimize the effects of base, solvent, temperature and amount of  $\text{SBA-Cu}^{2+}$ .

Table 2. Optimization of Suzuki coupling reaction over the  $\text{SBA-Cu}^{2+}$  nano catalyst.

Entry	Solvent	Base	Catalyst [mg]	Temp [°C]	Time [min]	Yield [%] <sup>a</sup>
1	PEG	$\text{Na}_2\text{CO}_3$	-	80	180	-
2	PEG	$\text{Na}_2\text{CO}_3$	4	80	120	trace
3	PEG	$\text{Na}_2\text{CO}_3$	5	80	60	15
4	PEG	$\text{Na}_2\text{CO}_3$	6	80	60	38
5	PEG	$\text{Na}_2\text{CO}_3$	7	80	60	58
6	PEG	$\text{Na}_2\text{CO}_3$	8	80	30	70
7	PEG	$\text{Na}_2\text{CO}_3$	9	80	30	85
8	PEG	$\text{Na}_2\text{CO}_3$	10	80	30	94
9	PEG	$\text{Na}_2\text{CO}_3$	11	80	30	95
10	PEG	$\text{NaHCO}_3$	10	80	30	81
11	PEG	$\text{NaOAc}$	10	80	30	35
12	PEG	$\text{KH}_2\text{PO}_4$	10	80	30	25
13	PEG	$\text{NaOH}$	10	80	30	-
14	PEG	$\text{K}_2\text{CO}_3$	10	80	30	-
15	$\text{H}_2\text{O}$	$\text{Na}_2\text{CO}_3$	10	80	30	78
16	Et-OH	$\text{Na}_2\text{CO}_3$	10	80	30	88
17	DMF	$\text{Na}_2\text{CO}_3$	10	80	30	15
18	DMSO	$\text{Na}_2\text{CO}_3$	10	80	30	trace
19	PEG	$\text{Na}_2\text{CO}_3$	10	25	180	-
20	PEG	$\text{Na}_2\text{CO}_3$	10	45	180	17
21	PEG	$\text{Na}_2\text{CO}_3$	10	60	30	45
22	PEG	$\text{Na}_2\text{CO}_3$	10	100	20	96

Reaction conditions: iodobenzene (1 mmol),  $\text{NaPh}_4\text{B}$  (0.5 mmol), PEG (2 mL), and 3 mmol base.

<sup>a</sup> Isolated yield

Unlike common boronic acid or esters, the prominent advantage of  $\text{NaBPh}_4$  is that it can react with four equivalents of electrophilic reagents. Therefore in aspect of economic and environmental concerns, this is a green protocol in organic synthesis. Despite this benefits, only a few works involving  $\text{NaBPh}_4$  for coupling reaction have been reported. Thus, to expand the scope and reactivity of sodium tetraphenyl borate, the development of new and efficient catalytic protocols is necessary [23].

Table 2 presents the results of optimization conditions. Firstly, 4 to 11 mg of catalyst was used to catalyze the model reaction at 80 °C in the presence of  $\text{Na}_2\text{CO}_3$  and PEG as solvent. The best result was obtained using 10 mg ( $0.379 \times 10^{-5} \text{ mol g}^{-1}$ ) of catalyst (Table 2, entry 8). While, there was no significant improvement in the reaction yield by increasing the amount of catalyst (Table 2, entry 9).

In order to find out the best base for this coupling reaction, the model reaction was evaluated in presence of  $\text{NaHCO}_3$ ,  $\text{NaOAc}$ ,  $\text{KH}_2\text{PO}_4$ ,  $\text{NaOH}$  and  $\text{K}_2\text{CO}_3$  (Table 2, entries 10–14). So the results were confirmed that  $\text{Na}_2\text{CO}_3$  is the best base among them. No product has been obtained in using of  $\text{NaOH}$  or  $\text{K}_2\text{CO}_3$  as a base. It seems that the strength of these base caused to the by-reactions.  $\text{NaOH}$  and  $\text{K}_2\text{CO}_3$  are the strongest base among other bases based on their  $K_b$  values. Knecht and co-workers [21] have reported that the amount of free and reactive  $\text{OH}^-$  for  $\text{KOH}$  or  $\text{NaOH}$  is higher than  $\text{Na}_2\text{CO}_3$  and  $\text{NaHCO}_3$  bases, which caused to a strong combination with metal species leading to a decrease in biphenyl yield. Therefore, it seems that high level of free hydroxide in entries 13 and 14 have strong combination with  $\text{Cu}$  species or strong reaction with  $\text{NaBPh}_4$  which caused to destroy the Suzuki reaction.

The effects of various solvents on the model reaction were studied by using Et-OH, DMSO,  $\text{H}_2\text{O}$  and DMF instead of PEG (Table 2, entries 15–18). The results show that the PEG was

Table 3. Suzuki–Miyaura coupling reaction with aryl halides and  $\text{NaPh}_4\text{B}$  catalyzed by  $\text{SBA-Cu}^{2+}$ .

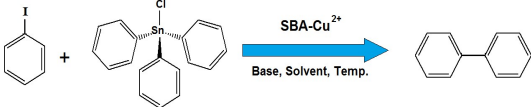
Entry	R	X	Time (min)	Yield [%] <sup>a</sup>	M.p. (°C)		TON	TOF ( $\text{h}^{-1}$ )
					Found	Reported		
1	H	I	30	94	68–69	68–70 <sup>[22]</sup>	248	496
2	4- $\text{CH}_3$	I	80	91	45–47	44–46 <sup>[22]</sup>	240	180
3	2- $\text{COOH}$	I	90	89	108–110	111–113 <sup>[2]</sup>	235	156
4	4- $\text{MeO}$	I	95	92	85–87	88–90 <sup>[22]</sup>	242	153
5	H	Br	40	90	68–69	68–70 <sup>[22]</sup>	237	355
6	4- $\text{NO}_2$	Br	160	92	111–113	112–114 <sup>[22]</sup>	242	91
7	4- $\text{CN}$	Br	180	91	83–84	85–86 <sup>[23]</sup>	240	80
8	4- $\text{Cl}$	Br	120	89	74–75	77–79 <sup>[22]</sup>	235	117
9	4- $\text{CH}_3$	Br	110	91	45–47	44–46 <sup>[22]</sup>	240	131
10	4- $\text{OH}$	Br	170	88	161–163	163–164 <sup>[23]</sup>	232	82
11	1-Br-naphthalene	Br	600	55	Colorless oil	Colorless oil <sup>[24]</sup>	145	14
12	H	Cl	360	64	66–69	68–70 <sup>[22]</sup>	168	28
13	4- $\text{CN}$	Cl	480	28 <sup>b</sup>	83–84	85–86 <sup>[23]</sup>	37	4.6
14	4-iodopyridine		40	86	66–68	69–70 <sup>[25]</sup>	227	325
15	4-bromopyridine		45	80	66–68	69–70 <sup>[25]</sup>	201	268

Reaction conditions: aryl halides (1 mmol), NaPh<sub>4</sub>B (0.5 mmol), PEG (2 mL), Na<sub>2</sub>CO<sub>3</sub> (3 mmol), SBA-Cu<sup>2+</sup> catalyst (10 mg, 0.379 mol%) and 80 °C.

<sup>a</sup>Isolated yield

<sup>b</sup>Containing 20 mg nano catalyst and 95 °C reaction temperature

Table 4. Optimization of Stille coupling reaction over the SBA-Cu<sup>2+</sup> nano catalyst.



Entry	Solvent	Base	Catalyst [mg]	Temp [°C]	Time [min]	Yield [%] <sup>a</sup>
1	PEG	Na <sub>2</sub> CO <sub>3</sub>	-	80	240	-
2	PEG	Na <sub>2</sub> CO <sub>3</sub>	4	80	60	trace
3	PEG	Na <sub>2</sub> CO <sub>3</sub>	5	80	50	14
4	PEG	Na <sub>2</sub> CO <sub>3</sub>	6	80	50	32
5	PEG	Na <sub>2</sub> CO <sub>3</sub>	7	80	50	54
6	PEG	Na <sub>2</sub> CO <sub>3</sub>	8	80	20	70
7	PEG	Na <sub>2</sub> CO <sub>3</sub>	9	80	20	81
8	PEG	Na <sub>2</sub> CO <sub>3</sub>	10	80	20	93
9	PEG	Na <sub>2</sub> CO <sub>3</sub>	11	80	20	94
10	PEG	NaHCO <sub>3</sub>	10	80	20	71
11	PEG	NaOAc	10	80	20	55
12	PEG	KH <sub>2</sub> PO <sub>4</sub>	10	80	20	43
13	PEG	K <sub>2</sub> CO <sub>3</sub>	10	80	20	18
14	H <sub>2</sub> O	Na <sub>2</sub> CO <sub>3</sub>	10	80	20	76
15	Et-OH	Na <sub>2</sub> CO <sub>3</sub>	10	80	20	89
16	DMF	Na <sub>2</sub> CO <sub>3</sub>	10	80	20	32
17	DMSO	Na <sub>2</sub> CO <sub>3</sub>	10	80	20	22
18	PEG	Na <sub>2</sub> CO <sub>3</sub>	10	25	240	trace
19	PEG	Na <sub>2</sub> CO <sub>3</sub>	10	45	120	52
20	PEG	Na <sub>2</sub> CO <sub>3</sub>	10	60	70	74
21	PEG	Na <sub>2</sub> CO <sub>3</sub>	10	100	15	95

Reaction conditions: Iodobenzene (1 mmol), triphenyltin chloride (0.5 mmol), PEG (2 mL), and 3 mmol base.  
<sup>a</sup>Isolated yield

more effective than other solvents. Despite aprotic solvents (DMSO and DMF), it seems that the protic solvents (PEG, Et-OH and H<sub>2</sub>O) have better effect on the coupling reaction catalyzed by SBA-Cu<sup>2+</sup>. It may be referred to the positive interactions between protic solvent and polar functional groups in SBA-Cu<sup>2+</sup> which can be help to effective dispersion.

In the other side, the

PEG as a phase transfer catalyst can enhance the solubility of the reagents (aryl halide, NaBPh<sub>4</sub>, base), as well as promote basicity of Na<sub>2</sub>CO<sub>3</sub>. The alcoholic solvent as a protic solvent have shown better yield than water because of its better polarity to dissolve reagents.

In continuous, it found that the reaction yields were impressionable to temperature factor. So, the effect of various temperature were studied in rang of 25 to 100 °C (Table 2, entries 19-22) and the best results were obtained at 80 °C (Table 2, entry 8). After optimizing the conditions, a series of aryl halides, which contain different substitution groups, such as electron-donating and electron-withdrawing were used for the synthesis of biphenyl derivatives in the presence of SBA-Cu<sup>2+</sup>. Table 3 shows the summarized results of this study in the optimized conditions (10 mg catalyst, Na<sub>2</sub>CO<sub>3</sub> as base in PEG solvent at 80 °C).

As expected, the Suzuki reaction for aryl iodides gave the best yields in the shorter times (Table 3, entries 1-4). Aryl bromides have shown high reactivity but relatively in longer reaction times versus aryl iodides (Table 3, entries 5-11). And regularly, the coupling of aryl chlorides were done in more difficult conditions that led to the lower yields (Table 3, entries 12-13). Overall, electronic effects have an effect on Suzuki reaction, so that aryl halides with electron-donating groups gave little higher yields than those with electron-withdrawing groups. Ortho-substituted aryl halides with (Table 3, entry 3) gave lower yields than those at para-substituted, which reveals that steric hindrance has a negative effect on the Suzuki reaction.

Table 5. Stille coupling reaction with aryl halides and triphenyltin chloride catalyzed by SBA-Cu<sup>2+</sup>.



Entry	R	X	Time (min)	Yield [%] <sup>a</sup>	M.p. (°C)		TON	TOF (h <sup>-1</sup> )
					Found	Reported		
1	H	I	20	93	68-69	68-70 <sup>[22]</sup>	245	735
2	4-CH <sub>3</sub>	I	120	90	45-47	44-46 <sup>[22]</sup>	237	118
3	2-COOH	I	125	89	108-110	111-113 <sup>[2]</sup>	235	113
4	4-MeO	I	100	86	85-87	88-90 <sup>[22]</sup>	227	136
5	H	Br	25	92	68-69	68-70 <sup>[22]</sup>	243	583
6	4-NO <sub>2</sub>	Br	75	90	111-113	112-114 <sup>[22]</sup>	237	190
7	4-CN	Br	80	91	83-84	85-86 <sup>[23]</sup>	240	180
8	4-Cl	Br	120	85	74-75	77-79 <sup>[22]</sup>	224	112
9	4-CH <sub>3</sub>	Br	100	89	45-47	44-46 <sup>[22]</sup>	235	141
10	4-OH	Br	120	87	161-163	163-164 <sup>[23]</sup>	229	114
11	1-Br-naphthalene	Br	420	59	Colorless oil	Colorless oil <sup>[24]</sup>	155	22
12	H	Cl	240	67	66-69	68-70 <sup>[22]</sup>	177	44
13	4-iodopyridine		30	88	66-68	69-70 <sup>[25]</sup>	222	443

14	4-bromopyridine	40	82	66-68	69-70 <sup>[25]</sup>	206	310
Reaction conditions: aryl halides (1 mmol), triphenyltin chloride (0.5 mmol), PEG (2 mL), Na <sub>2</sub> CO <sub>3</sub> (3 mmol), SBA-Cu <sup>2+</sup> catalyst (10 mg, 0.379 mol%) and 80 °C.							
<sup>a</sup> Isolated yield							

Table 6. Comparison of SBA-Cu<sup>2+</sup> nano catalyst for the Suzuki-Miyaura reaction with previously reported heterogeneous catalysts.

Entry	Substrate	Reagent	Catalyst type	Cu mol%	Time (min)	Temp (°C)	Yield (%)	Ref.
1	Ph-I	Ph-B(OH) <sub>2</sub>	Fe <sub>3</sub> O <sub>4</sub> @SiO <sub>2</sub> -Isatin-Cu <sup>2+</sup>	0.82	300	70	92	[6]
2	Ph-I	Ph-B(OH) <sub>2</sub>	Cu nano colloid	2	360	110	62	[7]
3	Ph-I	Ph-B(OH) <sub>2</sub>	3D MOF {[Cu(4-tba) <sub>2</sub> ](solvent)} <sub>n</sub>	-	-	25	88	[8]
4	Ph-I	Ph-B(OH) <sub>2</sub>	Cu-Pd@4A molecular sieve	9	60	78	99	[9]
5	Ph-I	Ph-B(OH) <sub>2</sub>	Cu@4A molecular sieve	9	60	78	62	[9]
6	Ph-I	Ph-B(OH) <sub>2</sub>	Pd-Cu/Carbon	0.99	180	78	97.5	[10]
7	Ph-Br	Ph <sub>4</sub> BNa	Pd <sup>2+</sup> @Polystyrene	1	18	120	90	[11]
8	Ph-I	Ph <sub>4</sub> BNa	SBA-Cu <sup>2+</sup>	0.379	30	80	94	This work
9	Ph-Br	Ph <sub>4</sub> BNa	SBA-Cu <sup>2+</sup>	0.379	40	80	90	This work

Using the hetero aryl halides (Table 3, entries 14, 15) shows the lower yields in compare with ordinary aryl halides these can be due to withdrawing effect of heteroatom in aryl halide. In order to demonstrate applications of the SBA-Cu<sup>2+</sup> as an active catalyst, it was evaluated in the C-C coupling through Stille reaction. Therefore, the reaction of iodobenzene and triphenyltin chloride were selected as a model reaction to obtain optimized conditions. In this way Table 4 shows the results of various conditions in model reaction. No product has been achieved without SBA-Cu<sup>2+</sup> catalyst (Table 4, entry 1). Similar to the Suzuki-Miyaura reaction, the best amount of nano catalyst were chosen 10 mg (0.379 × 10<sup>-5</sup> mol g<sup>-1</sup>) of the SBA-Cu<sup>2+</sup> (Table 4, entry 8). No significant improvement in yield was detected through increasing the amount of the SBA-Cu<sup>2+</sup> (Table 4, entry 9). Using the various base in the model reaction indicated that sodium carbonate was still the more efficient base among them (Table 4, entries 10-13).

In continuous, evaluation of various solvents in model reaction confirmed that the PEG is the best and effective solvent among them (Table 4, entries 14-17). As previously mentioned, PEG as a protic solvent have acted as phase transfer catalyst. Also ethanol as a protic solvent have shown better yield than water because of its better polarity to dissolve reagents. Finally, the temperatures in ranging from 25 to 100 °C were chosen to evaluate of the temperature effect in model reaction (Table 4, entries 8, 18-21). It was found that the reaction catalyzed effectively at 80 °C (Table 4, entry 8). As mentioned above, the best results are obtained with 10 mg (0.379 mol%) of SBA-Cu<sup>2+</sup> in PEG solvent at 80 °C and using Na<sub>2</sub>CO<sub>3</sub> (Table 4, entry 8). After optimization the reaction, various aryl halides with triphenyltin chloride were employed in Stille reaction for the synthesis of biphenyl derivatives. Table 5 summarized the results of this study. These results reveal that various aryl halides with electron-donating and electron-withdrawing substituents were catalyzed equally facile by SBA-Cu<sup>2+</sup> in appropriate yields and lower times. As expected aryl iodides

and bromides reacted in shorter times in compared to aryl chlorides.

Also in Stille reaction, using the hetero aryl halides (Table 5, entries 13, 14) indicates the moderate yields in compare with ordinary aryl halides these can be due to withdrawing effect of heteroatom in aryl halide.

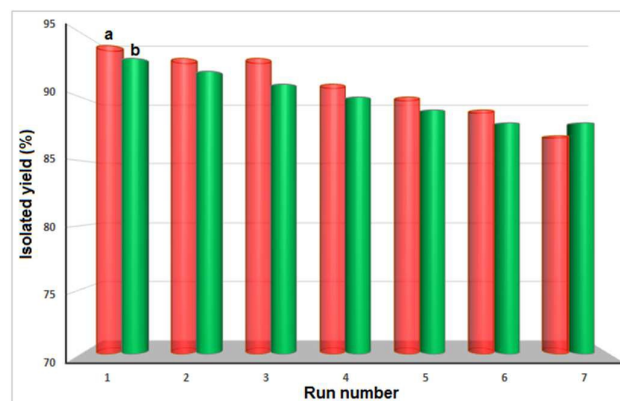


Fig. 10. Recycling and reusability of SBA-Cu<sup>2+</sup> in the coupling reaction of iodobenzene (1 mmol) with (a) NaBPh<sub>4</sub> (0.5 mmol) and (b) Ph<sub>3</sub>SnCl (0.5 mmol)

### 2.3. Copper content of nano catalyst

Inductively coupled plasma-optical emission spectrometry (ICP-OES) have been used to evaluate the amount of loaded Cu<sup>2+</sup> on SBA-Cu<sup>2+</sup>. The results indicated the value of 37.9 × 10<sup>-5</sup> mol g<sup>-1</sup> (2.41 %w Cu) in the nano catalyst sample. A hot filtration test was also performed to confirm the heterogeneous nature of the SBA-Cu<sup>2+</sup>. The nano catalyst was separated by hot filtration after the first catalytic reaction. Then the fresh reagents (Iodobenzene, NaPh<sub>4</sub>B, PEG and Na<sub>2</sub>CO<sub>3</sub>) were added to the hot filtrated solution. The resulting mixture was kept in reaction conditions (80 °C) for another 60

min. The conversion was negligible after adequate time (8 h). The negligible conversion in the amount of product indicated that copper leaching from SBA-Cu<sup>2+</sup> is very insignificant for coupling reaction.

#### 2.4. Reusability of catalyst

The reusability and recovery of the nano catalyst are very important factors in aspect of commercial applications. Hence, SBA-Cu<sup>2+</sup> separated by centrifugation after completion of reaction. Then the catalyst washed several times with water and methanol and dried in oven. The recovered catalyst can be reutilized for next reactions including the Suzuki-Miyaura and Stille. The reusability studies indicated that SBA-Cu<sup>2+</sup> can be recovered and reused without noticeable decline in its reactivity at least for seven runs. Fig. 10 shows that the average isolated yields for Suzuki and Stille reaction in seven runs are 91 and 90.14% respectively.

#### 2.5. Catalyst comparison

In order to show the activity of SBA-Cu<sup>2+</sup>, Table 6 presents the comparison of our results on the Suzuki reaction with the reported catalysts in the literature. There are limited number of reports about copper catalyzed Suzuki reactions. This comparison indicates that SBA-Cu<sup>2+</sup> is comparable or may be efficient than the other reported heterogeneous catalysts. Moreover, SBA-Cu<sup>2+</sup> is can be better than the other catalysts in terms of price, stability and toxicity.

### 3. Conclusion

In summary, SBA-Cu<sup>2+</sup> as a new mesoporous nano catalyst was fabricated and characterized. The characterization results confirmed the synthesized Schiff-base alumoxane support with nano flakes morphology formed the stable framework for Cu<sup>2+</sup> which can be thermally stable up to 306 °C. Also the copper percentage in nano catalyst were indicated (2.41 w%; 37.9 × 10<sup>-5</sup> mol g<sup>-1</sup>). The SBA-Cu<sup>2+</sup> showed significant catalytic activity and high reusability for the Suzuki-Miyaura and Stille reactions. This nanocatalyst is effective for reaction of various aryl halides (including chlorides, bromides and iodides) with NaBPh<sub>4</sub> and Ph<sub>3</sub>SnCl. In addition, this nanocatalyst could be recovered and reused at least for seven times without significant loss of catalytic activity. Copper leaching from SBA-Cu<sup>2+</sup> is very negligible for this coupling reaction.

### 4. Experimental

#### 4.1. Reagents and materials

Copper (II) acetate, aluminum nitrate [Al(NO<sub>3</sub>)<sub>3</sub>·9H<sub>2</sub>O] and other chemical reagents were purchased from Merck, Sigma-Aldrich, Fluka and Fisher chemical companies. All solvents and reagents were of analytical grade and used for the reaction without further purification. The powder XRD were recorded on a Philips PW 3040 X-ray diffractometer with Cu K $\alpha$  radiation ( $\lambda$ =1.5406 Å) in a range of 0.5–100° (Bragg's angle). Scanning electron micrographs (SEM) of the samples were recorded using FE-SEM MIRA3 TESCAN (acceleration voltage 30 kV). This microscope equipped with an energy dispersive X-ray detector (EDS) which used for chemical composition analysis and preparation of X-ray map of the nano catalyst. Transmission electron micrographs (TEM) were collected by a JEOL-2100 microscope. Fourier-transform infrared (FTIR) spectra were taken on Bruker alpha (German) with KBr pellets. TG-DTA

analysis was performed with STA PT-1000 instrument in the thermal range of 15-700 C with 11 mg of the samples (heating rate of 10 °C min<sup>-1</sup> under N<sub>2</sub> atmosphere). Nitrogen sorption and surface area measurement was carried on a Belsorp mini II analyzer at 77 K.

Prior to the analysis, degassing was done for all samples at 373 K in a vacuum line for 5 h. <sup>1</sup>H NMR spectra were recorded on a Bruker AVANCE DPX-400 (400 MHz for <sup>1</sup>H). Chemical shifts are given in ppm ( $\delta$ ) relative to internal TMS and coupling constants are reported in Hz. The Cu content of the catalyst was measured with an inductively coupled plasma atomic emission spectrometer (ICP-OES simultaneous, Varian VISTA-PRO Model). The ultrasonic bath (240 W-35 kHz, SONREX, DT52 H, Bandelin, Germany) has been utilized for ultrasonication of solutions.

#### 4.2. Catalyst preparation

##### 4.2.1. Synthesis of Boehmite (Bo)

Boehmite nanoparticles (Bo) were prepared according to the previously reported work [14]. Briefly, 50 mL NaOH solution 3.25 M and 30 mL aluminum nitrate [Al(NO<sub>3</sub>)<sub>3</sub>·9H<sub>2</sub>O] solution 1.77 M were prepared. The Al<sup>3+</sup> solution was then slowly precipitated with NaOH solution (2.94 mL min<sup>-1</sup>) by vigorous stirring. Then obtained milky mixture was sonicated in the ultrasonic bath for 3 h at the ambient temperature, filtered and washed with distilled water. The gelatinous precipitate was heated in the oven at 220 °C for 4 h.

##### 4.2.2. Synthesis of Schiff-base (SB)

Schiff base (SB) was prepared according to previous literature [26]. In brief, 0.1 mol salicylaldehyde was added to a stirred solution of 4-aminobenzoic acid (0.1 mol in 100 mL ethanol) and the mixture was stirred for 30 min at ambient temperature. The yellow precipitate of schiff-base was filtered and recrystallized with methanol to obtain SB.

##### 4.2.3. Synthesis of Schiff-Base Alumoxane (SBA) framework

2 g Boehmite (Bo) nanoparticles added to the stirred Schiff-base solution (0.266 g SB in 50 mL DMF), then the obtained mixture was refluxed for 17 h. After completion, the yellow precipitate of Schiff-Base alumoxane was separated by filtration and washed thoroughly by ethanol and methanol, and dried at 70 °C.

##### 4.2.4. Synthesis of Cu<sup>2+</sup>-Schiff-Base Alumoxane (SBA-Cu<sup>2+</sup>)

At the Erlenmeyer flask, 0.25 g of SBA and 0.1 g Copper (II) acetate were mixed into 50 mL ethanol. Then lid of the flask was closed and stirred for 24 h at room temperature. After completion, the blue-green mixture was filtered and washed several time with ethanol to obtain SBA-Cu<sup>2+</sup>. The resulting green catalyst (Fig. 1) was dried in oven at 60 °C.

#### 4.3. General procedure for Suzuki-Miyaura reaction

A mixture of aryl halides (1 mmol), NaPh<sub>4</sub>B (0.5mmol), Na<sub>2</sub>CO<sub>3</sub> (3 mmol), SBA-Cu<sup>2+</sup> nano catalyst (10 mg) and 2 mL solvent (PEG) were added to a test tube equipped with a magnetic stirrer bar. Until the completion of reaction, the mixture was heated at 80 °C and monitored by TLC to evaluate progress of reaction. After completion, the mixture was cooled down and catalyst was filtered off. Then separated catalyst washed several times via acetone and dried in oven. In a separating funnel, diethyl ether (4mL, 4 times) was utilized to extraction

## Paper

## RSC Advances

of organic phase from PEG filtrate by aid of adding water. At the end, the diethyl ether was evaporated in order to obtain corresponding biaryl product. The melting point of the final products were measured at the end. The biaryl products were characterized by  $^1\text{H}$  NMR spectra. The selected  $^1\text{H}$  NMR data for compounds 1 and 6 are in good agreement with those previously reported.

**1,1'-Biphenyl:**  $^1\text{H}$  NMR (400 MHz,  $\text{CDCl}_3$ ):  $\delta_{\text{H}}$  (ppm) = 7.62-7.64 (m, 4H), 7.40-7.50 (m, 4H), 7.36-7.40 (tt,  $J=7.6$ , 1.2 Hz, 2H).

**4-Nitro-1,1'-biphenyl:**  $^1\text{H}$  NMR (400 MHz,  $\text{CDCl}_3$ ):  $\delta_{\text{H}}$  (ppm) = 8.31-8.34 (dt,  $J=8.8$ , 2.4 Hz, 2H), 7.75-7.78 (dt,  $J=8.8$ , 2.4 Hz, 2H), 7.64-7.67 (m, 2H), 7.50-7.55 (m, 2H), 7.45-7.49 (tt,  $J=7.6$ , 2.4 Hz, 1H).

#### 4.4. General procedure for Stille reaction

A mixture of aryl halides (1 mmol),  $\text{Ph}_3\text{SnCl}$  (0.5 mmol),  $\text{Na}_2\text{CO}_3$  (3 mmol), SBA-Cu $^{2+}$  nano catalyst (10 mg) and 2 mL solvent (PEG) were added to a test tube equipped with a magnetic stirrer bar. Until the completion of reaction, the mixture was heated at 80 °C and monitored by TLC to evaluate progress of reaction. After completion, the mixture was cooled down and catalyst was filtered off. Then separated catalyst washed several times via acetone and dried in oven. In a separating funnel, diethyl ether (4mL, 4 times) was utilized to extraction of organic phase from PEG filtrate by aid of adding water. At the end, the diethyl ether was evaporated in order to obtain corresponding biaryl product. The melting point of the final products were measured at the end. The biaryl products were characterized by  $^1\text{H}$  NMR spectra. The selected  $^1\text{H}$  NMR data for compounds 2 and 7 are in good agreement with those previously reported.

**4-Methyl-1,1'-biphenyl:**  $^1\text{H}$  NMR (400 MHz,  $\text{CDCl}_3$ ):  $\delta_{\text{H}}$  (ppm) = 7.63-7.65 (m, 2H), 7.55-7.57 (m, 2H), 7.46-7.52 (m, 2H), 7.36-7.40 (tt,  $J=7.2$ , 1.2 Hz, 1H), 7.30-7.32 (d,  $J=8$  Hz, 2H), 2.46 (s, 3H).

**[1,1'-Biphenyl]-4-carbonitrile:**  $^1\text{H}$  NMR (400 MHz,  $\text{CDCl}_3$ ):  $\delta_{\text{H}}$  (ppm) = 7.74-7.77 (m, 2H), 7.69-7.72 (m, 2H), 7.60-7.63 (m, 2H), 7.49-7.53 (m, 2H), 7.43-7.47 (m, 1H).

#### Acknowledgements

Authors thank Ilam University and Iran National Science Foundation (INSF) for financial support of this research project.

#### References

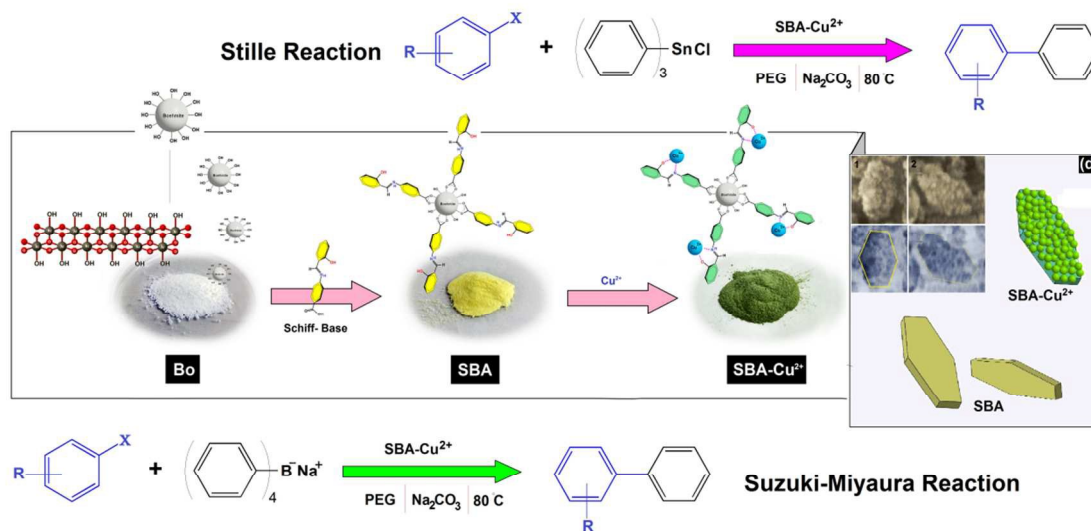
- (a) A. M. Trzeciak and J. Ziolkowski, *J. Coord. Chem. Rev.*, 2005, **249**, 2308-2322; (b) V. Farina, *Adv. Synth. Catal.*, 2004, **346**, 1553-1582; (c) B. M. Choudary, S. Madhi, N. S. Chowdari, M. L. Kantam and B. Sreedhar, *J. Am. Chem. Soc.*, 2002, **124**, 14127-14136; (d) A. Haberli and C. Leumann, *J. Org. Lett.*, 2001, **3**, 489-492.
- (a) M. Tobisu, T. Xu, T. Shimasaki and N. Chatani, *J. Am. Chem. Soc.*, 2011, **133**, 19505; (b) J. H. Li, Y. Liang and Y. Y. Xie, *Tetrahedron.*, 2005, **61**, 7289; (c) A. Ghorbani-Choghamarani and M. Norouzi, *Appl. Organometal. Chem.*, 2016, **30**, 140-147.
- (a) B. C. Makhubela, A. Jardine and G. S. Smith, *Appl. Catal. A-Gen.*, 2011, **393**, 231-241; (b) N. Iranpoor, H. Firouzabadi, S. Motevalli and M. Talebi, *J. Organomet. Chem.*, 2012, **708**, 118-124.
- J. Mao, J. Guo, F. Fang and S. J. Ji, *Tetrahedron.*, 2008, **64**, 3905-3911.

- (a) V. Calo, A. Nacci, A. Monopoli, E. Ieva and N. Cioffi, *Org. Lett.*, 2005, **7**, 617-620; (b) Y. Liu, D. Li and C. M. Park, *Angew. Chem. Int. Ed.*, 2011, **50**, 7333-7336; (c) N. Gigant and I. Gillaizeau, *Org. Lett.*, 2012, **14**, 3304-3307.
- S. S. Miri, M. Khoobi, F. Ashouri, F. Jafarpour, P. R. Ranjbar and A. Shafiee, *Turk. J. Chem.*, 2015, **39**, 1232-1246.
- M. B. Thathagar, J. Beckers and G. Rothenberg, *J. Am. Chem. Soc.*, 2002, **124**, 11858-11859.
- B. Wang, P. Yang, Z. W. Ge and C. P. Li, *Inorg. Chem. Commun.*, 2015, **61**, 13-15.
- A. Fodor, Z. Hell and L. Pirault-Roy, *Appl. Catal. A-Gen.*, 2014, **484**, 39-50.
- S. J. Kim, S. D. Oh, S. Lee and S. H. Choi, *J. Ind. Eng. Chem.*, 2008, **14**, 49-456.
- (a) B. Karimi and P. Fadavi Akhavan, *Chem. Commun.*, 2011, **47**, 7686; (b) S. Rostamnia and H. Xin, *Appl. Organomet. Chem.*, 2013, **27**, 348; (c) R. Zhang, W. Ding, B. Tu and D. Zhao, *Chem. Mater.*, 2007, **19**, 4379; (d) S. Mandal, D. Roy, R.V. Chaudhari and M. Sastry, *Chem. Mater.*, 2004, **16**, 3714; (e) C. D. Wu, A. Hu, L. Zhang and W. B. Lin, *J. Am. Chem. Soc.*, 2005, **127**, 8940; (f) X. Pan, Z. Fan, W. Chen, Y. Ding, H. Luo and X. Bao, *Nat. Mater.*, 2007, **6**, 507; (g) E. Castillejos, P.J. Debouttiere, L. Roiban, A. Solhy, V. Martinez, Y. Kihn, O. Ersen, K. Philippot, B. Chaudret and P. Serp, *Angew. Chem. Int. Ed.*, 2009, **48**, 2529; (h) L. Bai and J. X. Wang, *Adv. Synth. Catal.*, 2008, **350**, 315.
- A. A. Derakhshan, L. Rajabi and H. Karimnezhad, *Powder. Technol.*, 2012, **225**, 156-166.
- (a) F. Surivet, T. M. Lam, J. P. Pascualt and C. Mai, *Macromolecules.*, 1992, **25**, 5742-5751; (b) G. M. Whitesides, J. P. Mathias and C.T. Seto, *Science.*, 1991, **254**, 1312-1319.
- L. Rajabi and A. A. Derakhshan, *Sci. Adv. Mater.*, 2010, **2**, 163-172.
- J. Liu, X. Liao and B. Shi, *Res. Chem. Intermed.*, 2014, **40**, 249-258.
- A. A. Derakhshan and L. Rajabi, *Powder. Technol.*, 2012, **226**, 117-129.
- S. J. Obrey and A. R. Barron, *Macromolecules.*, 2002, **35**, 1499-1503.
- C. C. Landry, N. Pappé, M. R. Mason, A. W. Apblett, A. N. Tyler, A. N. MacInnes and A. R. Barron, *J. Mater. Chem.*, 1995, **5**, 331-341.
- S. A. Abdel-Latif, H. B. Hassib and Y. M. Issa, *Spectrochim. Acta. A.*, 2007, **67**, 950-957.
- B. Wang, X. L. Wu, C. Y. Shu, Y. G. Guo and C. R. Wang, *J. Mat. Chem.*, 2010, **20**, 10661-10664.
- D. B. Briggs, R. T. Pekarek and M. R. Knecht, *J. Phys. Chem. C*, 2014, **118**, 18543.
- Y. Y. Peng, J. Liu, X. Lei and Z. Yin, *Green Chem.*, 2010, **12**, 1072.
- L. Bai and J. X. Wang, *Adv. Synth. Catal.*, 2008, **350**, 315.
- E. H. Binns and K. H. Squire, *Trans. Faraday Soc.*, 1962, **58**, 762-770.
- B. J. Haworth, I. M. Heibron and D. H. Hey, *J. Chem. Soc.*, 1940, 349.
- Y. Leng, J. Liu, C. Zhang and P. Jiang, *Catal. Sci. Technol.*, 2014, **4**, 997-1004.

## Graphical Abstract

## Copper-Schiff base alumoxane: a new and reusable nanocatalyst for Suzuki–Miyaura and Stille C-C cross-coupling reactions

Arash Ghorbani-Choghamarani,\* Maryam Hajjami, Ali Ashraf Derakhshan and Laleh Rajabi



For the first time, Cu(II) supported on Schiff-base alumoxane framework was used as an effective and recyclable nanocatalyst in Suzuki-Miyaura and Stille cross coupling reactions.